Applied Thermal Engineering 88 (2015) 22–32

Contents lists available at ScienceDirect

Applied Thermal Engineering

journal homepage: www.elsevier.com/locate/apthermeng

Investigations on heat transfer characteristic of molten salt flow in helical annular duct

Peng Xiao, Liejin Guo*, Ximin Zhang

State Key Laboratory of Multiphase Flow in Power Engineering, Xi'an Jiaotong University, Xi'an 710049, China

HIGHLIGHTS

- A molten salt double tube helical heat exchanger was built.
- Nusselt number of molten salt flow in helical annular duct was experimental obtained.
- The molten salt flow regimes could be distinguished by Darcy friction factor.
- Higher heat transfer enhancement ratio was found with decreasing molten salt temperature.
- Smaller inner–outer-pipe diameter ratio leads to higher heat transfer enhancement ratio.

ARTICLE INFO

Article history:
Received 3 June 2014
Received in revised form
15 August 2014
Accepted 6 September 2014
Available online 16 September 2014

Keywords:
Molten salt
Heat exchanger
Heat storage

ABSTRACT

Molten salt is a preferable heat storage and heat transfer media, which can be employed in the high temperature industrial applications. A novel double tube helical heat exchanger (DTHHE) was developed in State Key Laboratory of Multiphase Flow in Power Engineering (SKLMF) using molten salt as the hot fluid flowing through the outer annular duct, to supply the heat for subcritical and supercritical water. In this work, the heat transfer characteristics of molten salt flow from laminar flow regime to turbulent flow regime were experimentally investigated. Heat transfer enhancement was detected in helical annular duct, and the enhancement ratio was found different from that in helical circular pipe. The heat transfer results were correlated separately in various flow regime, and the divergences between correlated equation and the classical heat transfer correlations of helical circular tube were analysed. The effects of inner tube surface were found pronounced on the flow and heat transfer characteristics. The experimental effort and results will benefit the design and operation of heat exchanger process between molten salt flow and water.

1. Introduction

A variety of fluids was employed in high temperature heat storage and transfer, including water, vapour, air, and mineral oil, before molten salt was considered as more preferable, within the temperature range from 300 °C to 600 °C. Profit from their favourable thermal physical and chemical properties at high temperature, such as large specific heat, low vapour pressure, low corrosive and toxic, chemical stability etc, molten salt was widely used in chemical, metallurgy and nuclear industries as an ideal heat transfer medium. In this work, the molten salt (KNO_3: 53%, $NaNO_2$: 40%, $NaNO_3$: 7%) was used to store solar thermal energy and transfer the absorbed heat to supercritical water for power generation or thermochemical utilization.

Because of many advantages of a helical coiled tube, such as high efficiency in heat transfer, compactness in structure, easy to manufacture, etc., a novel double tube helical heat exchanger using molten salt as a hot heat transfer medium was proposed, which was successfully constructed at the State Key Laboratory of Multiphase Flow in Power Engineering.

The issue of fluid flow and heat transfer in curved pipe was widely concerned. Dean [1] (1928) proposed a dimensionless flow parameter, called Dean number, for assessing the effect of centrifugal force in a curved tube. It was reported that the presence of centrifugal force due to the curvature will lead to a significant radial pressure gradient in the flow core region, and then two symmetrical vortexes (secondary flow) are generated when the Dean number exceeds a critical number.

* Corresponding author. Tel.: +86 29 8266 3895; fax: +86 29 8266 9033.
E-mail address: lj-guo@mail.xjtu.edu.cn (L. Guo).

http://dx.doi.org/10.1016/j.applthermaleng.2014.09.021
1359-4311/

$$De = Re(d/D_H)^{1/2} \quad (1)$$

In this work, the thermal equivalent diameter d in annular duct was obtained according to Kays's theory [2]. The calculation equations of d were listed in the Nomenclature. After the pioneer work of Dean [1], many investigations have been conducted regarding flow in curved and helical tubes. The heat transfer and frictional pressure drop characteristics of steady flow in curved tube have been studied by numerous work, both theoretically and experimentally. Seban et al. [3] experimentally investigated the laminar and turbulence flow in curved tube respectively. The entry effect for laminar flow was found significant on heat transfer rate, while it has little impact for turbulent flow. For unsteady flow in curved pipe, Mori et al. [4,5] analysed the flow field in curved tube for fully developed laminar flow, and divided the flow region into the core region and the boundary layer region along the wall. The mechanisms of heat transfer enhancement and additive flow resistance were deduced by theoretically analysis. Guo et al. [6] performed an investigation of the effects of pulsation upon transient convective heat transfer characteristics in a uniformly heated helical coiled tube. The secondary flow mechanism and the effect of interaction between the flow oscillation and secondary flow were analysed. A series of new correlations of the average and local heat transfer coefficients were proposed under steady and oscillatory conditions.

In the previous experiments, water, air or oil were used as a heat transfer medium, which have little temperature-dependent thermal physical properties, thus little deviation was generated when the fluid was postulated as constant thermal property.

Fig. 1 shows the thermal physical properties of ternary nitrate molten salt (KNO_3:$NaNO_3$:$NaNO_2$ = 53:7:40). When the molten salt is heated beyond the melting point, solid-to-liquid phase change occurred. Then molten salt becomes oil like fluid with high viscosity at low temperature region (150 °C–300 °C). The molten salt had a high Prandtl number ($Pr > 7$) and poor fluidity, which means that the thickness of the velocity boundary layer was much bigger than the thermal boundary layer, thus secondary flow in curved tube was very effective for enhancing the heat transfer process. With the increasing temperature, the viscosity and Prandtl number decrease, and the molten salt transforms into water-like liquid. The Prandtl number of the molten salt in high temperature region (300 °C–500 °C) is close to that of ordinary condition water: around the number of 7. The molten salt at the temperature of 300 °C–500 °C has favourable fluidity and thin velocity boundary layer. The ratio of the molten salt's velocity thermal boundary layer to thermal boundary layer is similar to that of ordinary condition water. Since the thermal physical properties of molten salt were more complex and sensitive to the temperature, the variations of thermal properties have to be considered for investigating the heat transfer characteristics.

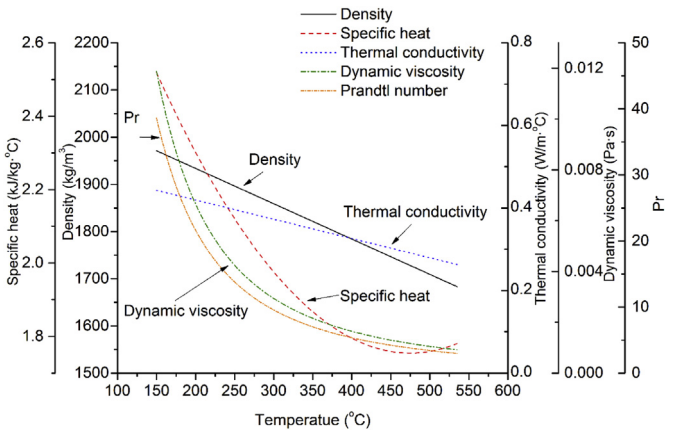

Fig. 1. Thermal physical properties of ternary nitrate molten salt.

The flow patterns in curved annular pipe are significantly different from those in a curved circular pipe because of the presence of the inner-wall boundary. Karahalios [7] proposed that secondary flow took the form of two pairs of vortices in the annular cross-section, which resulted in differences on heat transfer coefficient and frictional pressure drop. Evolution of the secondary flow and the effect of radius ratio on the flow patterns were discussed by Choi et al. [8]. The heat transfer correlations for laminar and transition flow were suggested in curved annular duct. Garimella et al. [9] studied the force convective heat transfer in coiled annular ducts. Hot and cold water were used as heat transfer fluids. The results revealed that the obtained heat transfer coefficients in the coiled annular duct were higher than those in a straight annular duct, especially in the laminar region. Xin et al. [10] investigated the pressure drop of single-phase and two-phase air–water flow in helical annular pipes. A friction factor correlation for single-phase flow in laminar, transition and turbulent flow regime was proposed. Kang et al. [11] studied the condensation heat transfer and pressure drop characteristics of refrigerant HFC-134a flowing in a helical coiled tube. The results showed that the tube-side heat transfer coefficients of the refrigerant decreased as shell-side water Reynolds number increased. Rennie et al. [12] experimentally reported the heat transfer characteristics in a coil-in-coil heat exchanger. The results showed that the flow in the inner tube with high inner-to-outer-pipe ratio was the limiting factor for the overall heat transfer coefficient. The effects of cooling wall temperature on the heat transfer coefficients were investigated. Correlations derived from the measurement data were proposed and compared with that of horizontal straight pipe.

However, to the author's best knowledge, few studies have been done for heat transfer and pressure drop characteristics in annular helical coiled duct, especially regarding property-variable molten salt. This work was primarily focus on the heat transfer and frictional pressure drop characteristics of molten salt fluid in the DTHHE. The characteristics of heat transfer and friction factor induced by secondary flow in curved annular duct were analysed. The correlations for average molten salt heat transfer coefficients were obtained within the laminar region to turbulent region. The present investigations will be helpful to the design and safe operation of molten salt heat exchanger.

2. Experimental system and method

2.1. Molten salt circulation system and test section

A novel system of molten salt heat transfer and a double-tube helical heat exchanger (DTHHE) were built at the State Key Laboratory of Multiphase Flow in Power Engineering (SKLMFPE) to study the molten salt heat transfer behaviours in a helical annular duct.

As shown in Fig. 2, the system consists of: i) a molten salt hot loop, ii) a water cold loop, and iii) a double tube helical heat exchanger (DTHHE). The molten salt hot loop was mainly composed of three components. A molten salt vessel with capacity of 300 L was constructed for heat the solid molten salt to liquid and storage the liquid molten salt. A submersible axial-pump with flow rate of 200–2000 L/h was developed for delivering molten salt fluid. An electrical preheater was used for handling the molten salt flow temperature at a desired value before it entered the heat transfer test section. The preheater was regulated by an automatic PID regulator. The mass flow rate of molten salt was measured by a

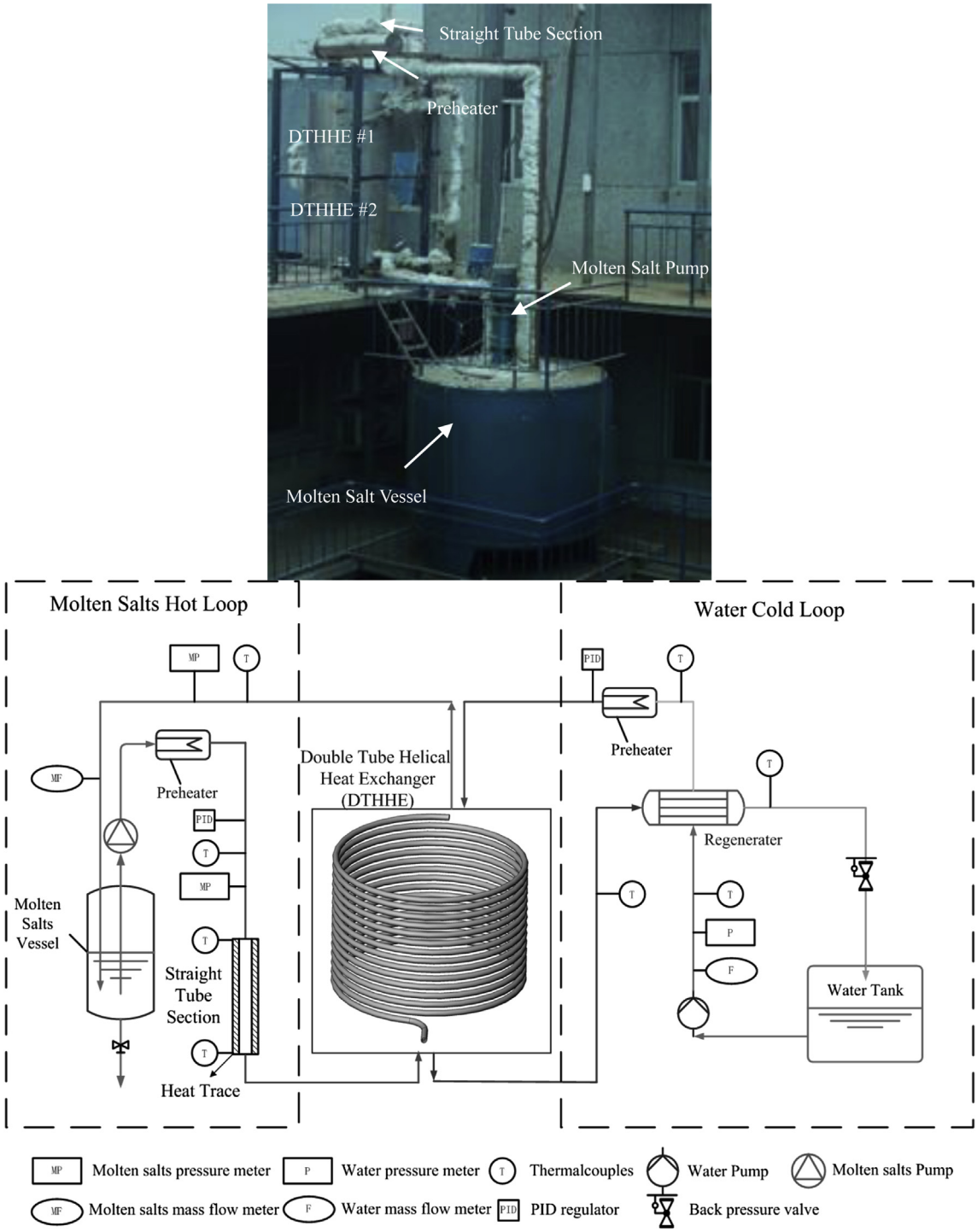

Fig. 2. Schematic of the experimental setup.

target type flow meter with a range of 200–2000 L/h. The generated signal was transmitted to an electrical transmitter to be displayed and stored.

The water cold loop included three parts: a water tank, a reciprocating plunger type pump and a regenerator. The water tank contained deionized water, which was pumped into the DTHHE inner tube. The reciprocating plunger type pump with the flow range of 2 to 12 L/h was used to transport the deionized water and increased the water pressure up to 25 MPa. The water loop's pressure was regulated by a back pressure valve and measured by a pressure meter at the outlet of plunger pump. A regenerator was employed to recycle thermal energy of the hot outflow water from the DTHHE. In the water loop, the DTHHE inlet temperature was controlled by an electrical preheater, which could maintain the water temperature at a desired point by adjusting input power. The mass flow of water flow rate was obtained by a Coriolis mass flow meter manufactured. The mass flow rate of water was set at 50–200 g/min.

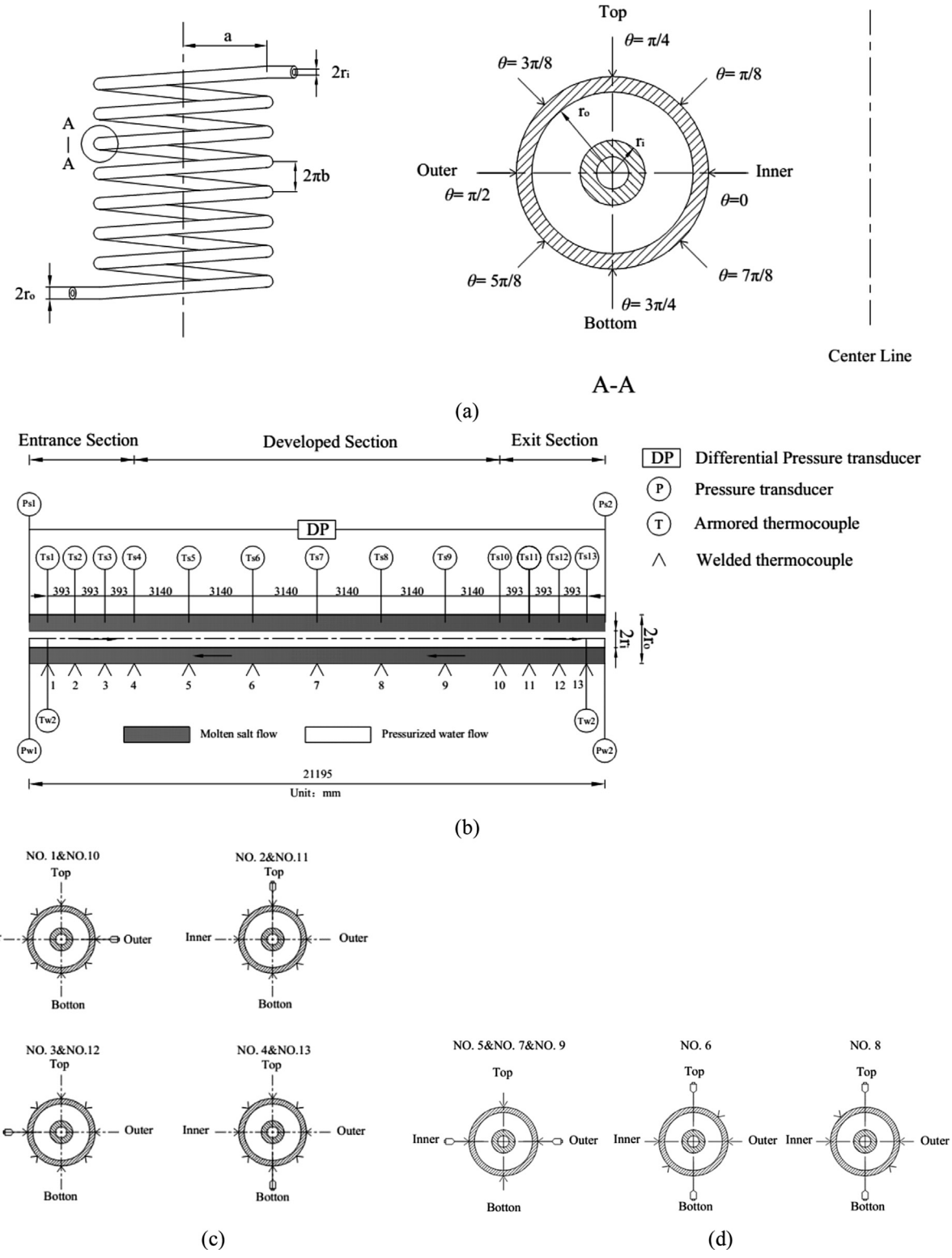

Fig. 3. Schematic diagram of the test section.

The molten salt heat transfer experiments in straight line were conducted for checking the validity of empirical molten salt heat transfer correlations in literature [13,14]. A straight tube test section with length of 1 m and inner diameter of 20 mm was arranged. The heat flux rates, wall temperatures as well as inlet and outlet molten salt flow temperatures were measured for heat transfer rate calculation. According to the comparisons of the heat transfer coefficients and friction factors in a helical annular duct and in a straight pipe, the heat transfer and frictional pressure drop characteristics of molten salt in helical annular duct were proposed.

As it is presented in Fig. 3, subcritical water and molten salt flows were parallelly and counter-currently arranged in DTHHE. In

axial direction, the effect of entrance and exit flow was taken into accounted. The test section was divided into three sub-sections: entrance section, developed section and exit section. Thirteen K-type armoured thermocouples and various welded thermocouples were fabricated on the coiled tube side to monitor the bulk and wall temperature of molten salt flow. Meanwhile, the inlet and outlet temperature of inner flow were obtained by two K-type thermocouples.

To investigate the influences of curvature ratio ($\alpha = d/D$) on heat transfer characteristics, two DTHHEs with different tube diameters were employed, and the structural and experimental parameters of these tested DTHHEs are indicated in Table 1.

In the present experiments, the mass flow rates of molten salt and water, water pressure, molten salt bulk temperature and outer wall temperatures of double tube exchanger were directly measured. The summary of uncertainties in this work was shown in Table 2.

2.2. Data acquisition

The energy balance of molten salt flow and water flow was as follow:

$$\Delta H_{MS} = Q_L + Q_T = h_o^i A_o^i \left(T_{MS} - T_o^i\right) + kA_i^o \Delta T_m \tag{2}$$

where ΔH_{MS} was the enthalpy variation of molten salt flow; Q_L and Q_T were heat loss flux through the outer helical pipe of DTHHE and heat transfer flux through the inner helical pipe of DTHHE, respectively; h_o^i and k were heat transfer coefficients on the inner wall of outer helical pipe and overall heat transfer coefficients between molten salt and water flow, respectively; A_o^i and A_i^o were the area of the inner wall of the outer pipe and the outer wall of the inner pipe, respectively; T_{MS}, T_o^i and ΔT_m denoted the molten salt mean temperature, the inner wall temperature of outer helical pipe and the modified logarithmic mean temperature difference between molten salt fluid and water, respectively.

According to the thermal resistances, the overall heat transfer coefficient could be related to the molten salt and water heat transfer coefficients by the following equation:

$$\frac{1}{k} = \frac{d_i^o}{h_i^i d_i^i} + \frac{d_i^o}{2\lambda_m} \ln\left(\frac{d_i^o}{d_i^i}\right) + \frac{1}{h_i^o} \tag{3}$$

where d_i^o and d_i^i denoted the outer diameter and inner diameter of the inner helical pipe, respectively; λ_m denoted the thermal conductivity of the inner helical tube; h_i^i denoted the heat transfer coefficient of water flow in inner helical pipe; h_i^o denoted the heat transfer coefficient of molten salt flow in the outer annular duct.

Table 1
The structural and experimental parameters of the DTHHEs.

	DTHHE #1	DTHHE #2
Inner-tube internal diameter (mm)	6	6
Outer-tube internal diameter (mm)	19	26
Double tube length (mm)	2500	2480
Coil diameter (mm)	530	530
Coil pitch (mm)	50	50
Water pressure (MPa)	0.1–30	0.1–30
Water mass flow rate (g min^{-1})	200–1000	200–1000
Molten salt volume flow rate (L min^{-1})	1–5	1–5
Water mass flux (kg m^{-2} s^{-1})	100–500	100–500
Molten salt mass flux (kg m^{-2} s^{-1})	300–1200	700–3000
Water-side Reynolds number	10,000–110,000	10,000–110,000
Molten salt Reynolds number	200–20,000	500–40,000

Table 2
The uncertainty summary of measurements and calculation processes.

Parameters	Uncertainty
Pressure (MPa)	1.5%
Tube length and duct diameter	1.0%
Mass flow rate of molten salt (kg/s)	1.5%
Mass flow rate of water (kg/s)	0.20%
Fluid temperature of molten salts (K)	1.1%
Fluid temperature of water (K)	1.1%
Wall temperature (K)	0.80%
Heat transfer coefficient (kW/(m^2 K))	6.4%

To avoid overheated steam flowing in the inner helical pipe, subcritical water ($P = 25$ MPa, $T = 200$ °C–372 °C) and supercritical water ($P = 25$ MPa, $T = 372$ °C–550 °C) were employed to absorb heat from molten salt fluid. For determining the heat transfer coefficient of supercritical water in the inner helical pipe, Mao's correlation [15] was adopted:

$$Nu = 0.0161 Re_b^{0.848} Pr_b^{0.632} (\rho_w/\rho_b)^{0.851}, \quad G = 80 \sim 1600 \text{ kg m}^{-2} \text{ s}^{-1} \tag{4}$$

The G was mass flux, defined as the ratio of mass flow rate to the cross-section area of flowing pipe.

For determining the heat transfer coefficient of subcritical water flow through inner helical pipe, Guo's correlation [6] and Seban's correlation [3] was used based on the Reynolds number of inner water in experiments:

$$Nu = 0.044 Re_b^{0.8} Pr_b^{0.4} De^{-0.0495}, \quad Re = 4 \times 10^4 \sim 3.5 \times 10^5 \tag{5}$$

$$Nu = 0.023 Re^{0.85} Pr^{0.4} \left(\frac{r}{a}\right)^{0.1}, \quad Re = 6000 \sim 65,600 \tag{6}$$

Before the heat transfer experiment, the heat loss flux of heat exchanger with various flow rates should be primarily determined. In this step, the molten salt was arranged to flow through the outer annular duct without water-cooling, with the same mass flow rate in heat transfer experiments between molten salt and water. The molten-salt temperature difference between inlet and outlet could be obtained, and the heat flux through the outer helical pipe of DTHHE could be calculated by the following equation:

$$\dot{q}_L = M_{MS}(H_{MS,o} - H_{MS,i})/A_o^o \tag{7}$$

where $\dot{q}_L$ was the heat flux through the outer pipe; M_{MS} was the mass flow rate of molten salt flow; $H_{MS,o}$ and $T_{MS,i}$ were inlet and outlet enthalpy of molten salt flow based on the inlet and outlet temperature, respectively.

The heat transfer coefficients of molten salt on inner surface of outer helical pipe could be obtained by solving Inverse Heat Conduction Problem [16]. According to the energy conservation, the governing equation for heat transfer through outer helical pipe were followings:

$$\frac{\partial}{\partial r}\left(\lambda r \frac{\partial T}{\partial r}\right) + \frac{\partial}{\partial \theta}\left(\frac{\lambda}{r}\frac{\partial T}{\partial \theta}\right) = 0 \tag{8}$$

$$\lambda \frac{\partial T}{\partial r} = \dot{q}_L(T), \quad r = r_o^o \tag{9}$$

$$\lambda \frac{\partial T}{\partial r} = h_o^i \cdot \left(T - T_b\right), \quad r = r_o^i \tag{10}$$

where (r, θ) was the position parameter in two-dimensional polar coordinates; T_b was the bulk temperature of molten salt flow; h_o^i was the heat transfer coefficient, which could be determined by the iteration computing the difference of measured outer temperature of outer pipe and the calculated temperature in the same position, until the difference was less than convergence factor. The iteration process and the value of convergence factor were shown in Fig. 4.

In the second step, the heat transfer characteristics of molten salt flow on the outer surface of inner helical pipe was mainly concerned, which determined the total heat transfer rate from molten salt to water. The heat transfer coefficient of molten salt was experimentally obtained using Wilson-Plot method [17]. It is theorized that if the mass flow of the molten salt flow was modified, then the change in the overall thermal resistance would be mainly determined by the variation of the variation of molten salt convection coefficient, meanwhile the remaining thermal resistances kept nearly constant. Thus the molten salt heat transfer coefficient could be obtained by measuring the variations of overall thermal resistance.

To promote the measurement precision of heat transfer coefficient, the effect of heat loss was evaluated with a new parameter called "heat loss temperature difference". According to the differential analysis of the heat transfer process with additional heat loss flux $\dot{q}_L$ on the outer surface of the outer pipe, the new parameter was defined as follows:

$$\varepsilon = \frac{\dot{q}_L \cdot (r_o^o / r_i^o)}{\eta k W_{MS}} = \frac{\dot{q}_L \cdot (r_o^o / r_i^o)}{k(1 - W_{MS}/W_W)},\ W = M \cdot \overline{C_p},\ \eta = \frac{1}{W_{MS}} - \frac{1}{W_W} \tag{11}$$

Then the modified logarithmic mean temperature difference was deduced by the following equations:

$$\mathrm{LMTD} = \frac{\Delta T_{max} - \Delta T_{min}}{\ln\left(\frac{\Delta T_{max}+\varepsilon}{\Delta T_{min}+\varepsilon}\right)} - \varepsilon,\quad k = \frac{Q_i}{A_i^o \cdot \mathrm{LMTD}} \tag{12}$$

The experimental process as well as calculation procedure were shown in Fig. 4, heat transfer coefficients of molten salt flow on the inner wall of the outer pipe and on the outer wall of the inner pipe were calculated separately.

For calculating the Darcy friction factor of molten salt in a helical annular duct, the inlet and outlet pressure as well as the pressure difference between inlet and outlet were experimentally measured with various molten salt velocity.

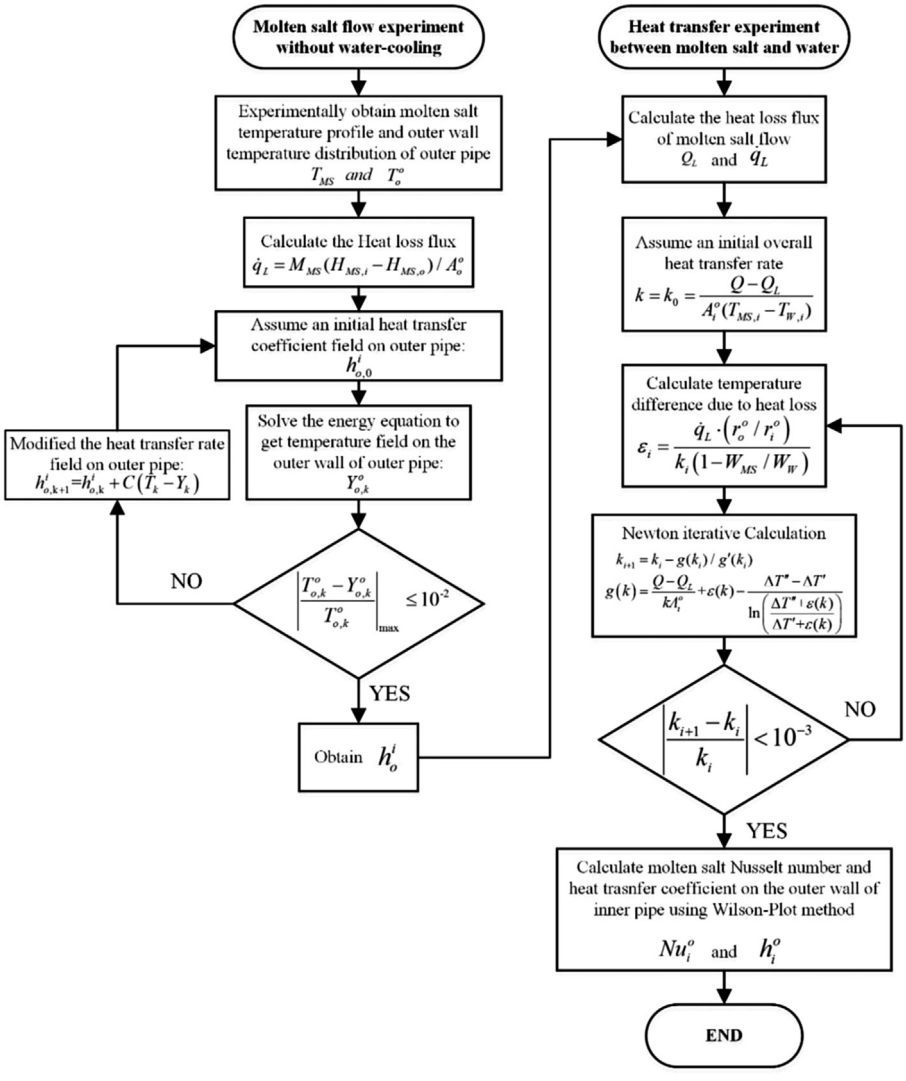

Fig. 4. Experimental and calculation procedure for heat transfer coefficients of molten salt flow.

$$f = \frac{(r_o^i - r_i^o)}{2\bar{\rho}\bar{u}^2 n\pi a}\left[\Delta P_c + 2\bar{\rho}gn\pi a\sin\left(\frac{b}{a}\right) - \frac{\rho_i}{\rho_o}u_i^2(\rho_i - \rho_o)\right] \quad (13)$$

where the $\bar{u}$ denoted the average velocity of molten salt flow in helical annular duct; $\bar{\rho}$ denoted the average density based on the average temperature between inlet and outlet; n and a denoted the coil number and coil radius, respectively; ΔP_c denoted the gauge pressure difference between inlet and outlet; b denoted the pitch of the helical coils.

3. Results and discussion

3.1. Frictional pressure drop and flow regime distinction

The Darcy friction factors of molten salt flow versus various Reynolds number were plotted in Fig. 5. It was found that for lower values of Reynolds number (up to 2×10^3), the Darcy frictional factor decreases as the Reynolds number increases. As the Reynolds number increased further, irregular pressure variation were detected, and the Darcy friction factors were enlarged suddenly. The phenomenon was stated by Liu et al. [18] as an onset of turbulence. Thus we considered this sudden increase in friction factor as the divide between laminar and turbulent flow regimes. When the sudden increase occurred, the Reynolds number was defined as the critical Reynolds number in this work.

For DTHHE #1, the critical Reynolds number was around 5500. For coil #2, the critical Reynolds number was about 4600. It was shown that the turbulent flow was delayed with the smaller inner tube diameter. Xin et al. [10] studied the transition process in helical annular pipe using water as working fluid. They found that the transition process from laminar regime to turbulent regime was governed by the drag effect of pipe walls. Besides, the different curvatures and areas of inner and outer wall led to different drag forces on the pipe flow, Thus different onsets of turbulence on the inner and outer wall were induced. In this work, the smaller inner tube diameter resulted in less wall area and less drag force on the molten salt flow. Thus flow in the DTHHE #1 seemed more stable than DTHHE #2 and transformed into turbulence with larger Reynolds number.

The critical number were little smaller than the predicted value of helical circular pipe proposed by Ito [19]:

$$Re_{cr} = 20,000 \times \left(\frac{d}{D_H}\right)^{0.32} \left(1.16 \times 10^{-3} < \frac{d}{D_H} < 0.067\right) \quad (14)$$

According to Ito's correlation, the critical Reynolds number was 6250 for DTHHE #1 and 4997 for DTHHE #2. The difference between the experimental data and prediction of (14) was not larger than 15%. The main difference of annular duct and circular pipe was that the annual duct has an additional inner tube surface, which caused a different vortex distribution on the cross-section of the duct. As it was pointed out by Petrakis [20], the inner tube surface could break the force balance of the pressure gradient and the centrifugal force acting on the fluid. The non-balance forces generate an additional pair of vortices (secondary flow) near the inner tube surface. The presence of two more vortices increases the flow instability and causes laminar flow transforming into turbulent flow earlier.

3.2. Heat transfer characteristics of laminar regime

The Nusselt number of laminar molten salt flow in helical annular duct was drawn in Fig. 6. It was shown that the Nusselt number on the inner wall of helical annular duct was higher than that of the outer wall. Both of them increased with the increasing Dean number. The reason was that the axial velocity gradient near the inner wall was higher than that near the outer wall. Furthermore, secondary flow generated vortices with stronger intensity adjacent to the inner wall than those near the outer wall. All of above factors enhanced the heat transfer rate on the inner wall.

Ghia et al. [21] proposed that the significant similarity parameter of flow in curved pipe was Dean number ($De = Re(d_T/D_H)^{0.5}$), rather than Reynolds number. Thus we used Dean number to represent the flow characteristics of molten salt in helical annular duct.

$$Nu_l = C_1 De^{C_2} Pr^{1/3} \quad (15)$$

Since the heat transfer process between molten salt and pressurized water was dominated and most concerned, here the Nusselt number of laminar flow regime on outer surface of inner helical pipe was correlated by the above equation (15), in which C_1 and C_2 were the coefficients to be determined by the experimental data.

In this work, two types of helical annular pipe were employed for investigating the heat transfer characteristics of molten salt. It was found that both the experimental data of different pipes could be correlated in the same equation as follows:

$$Nu_l = 0.836 De^{0.487} Pr^{1/3}, \quad 250 < De < 1000, \quad Pr > 1 \quad (16)$$

The deviations between the correlated value and experimental data were drawn in Fig. 6(b) and (d) for DTHHE #1 and DTHHE #2, respectively. The deviations were found less than ±20% in the region of $250 < De < 1000$, which indicated that the correlation has a

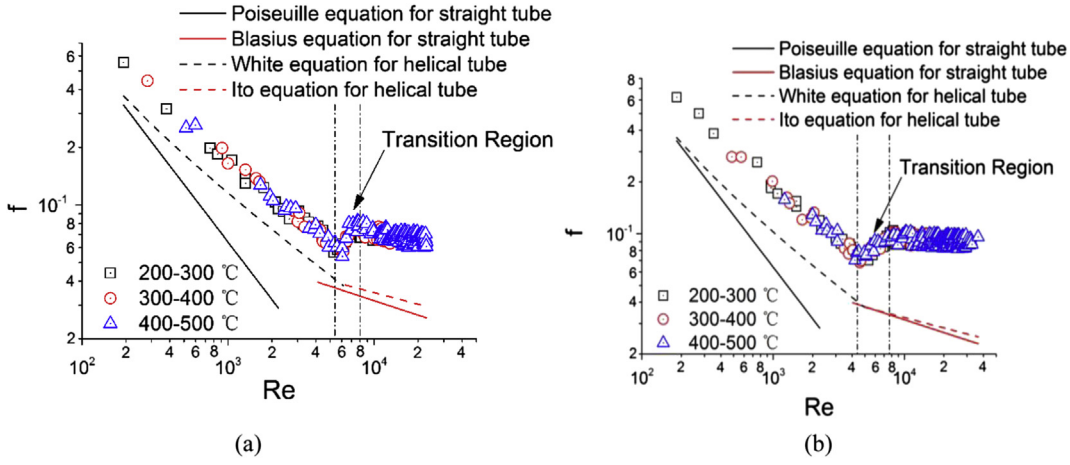

Fig. 5. The Darcy frictional factor with different Reynolds number: (a) DTHHE #1; (b) DTHHE #2.

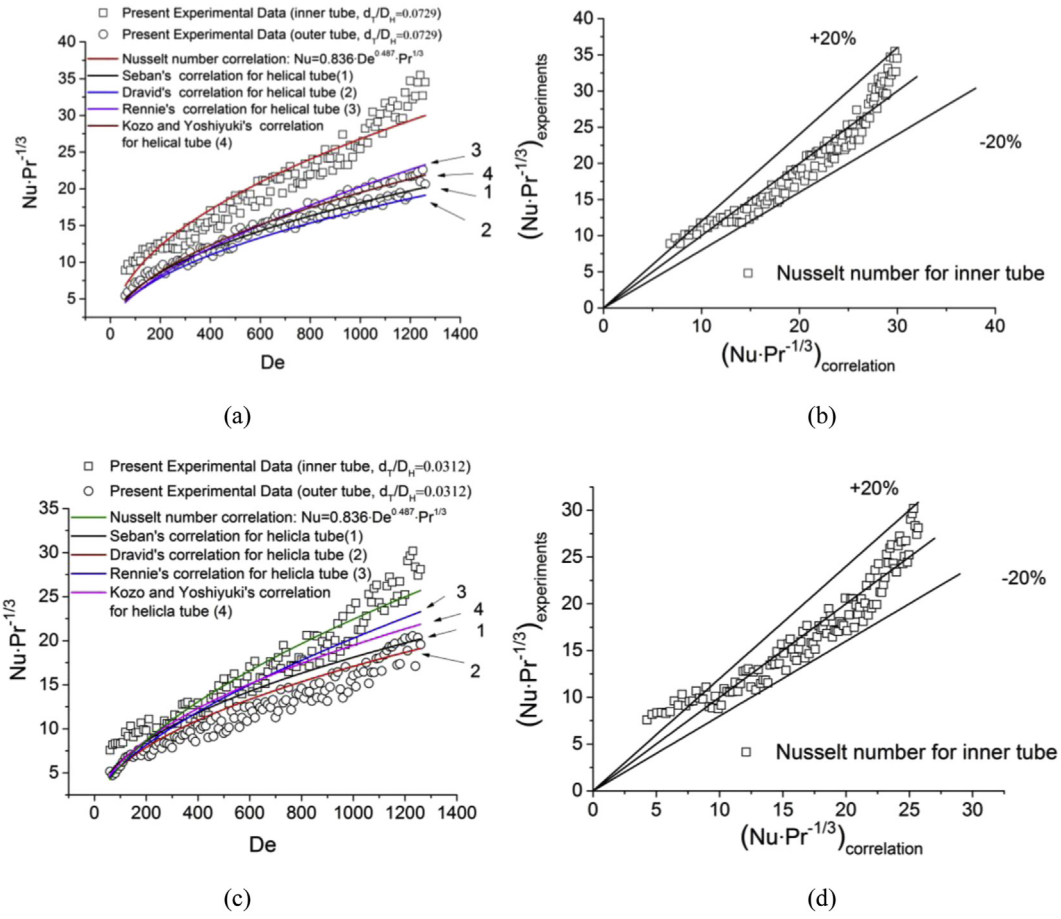

Fig. 6. The laminar Nusselt numbers on inner and outer surface of helical annular duct versus various Dean number: (a) Nusselt number of DTHHE #1; (b) Deviation analysis for *Nu* correlation of DTHHE #1; (c) Nusselt number of DTHHE #2; (d) Deviation analysis for *Nu* correlation of DTHHE #2.

good accuracy for laminar molten salt flow regime. The undervalued correlated value in $De < 250$ was induced by the natural convection effect, which could not be ignored when the velocity of molten salt flow was small. The natural convection could enhance the heat transfer coefficients in laminar flow regime.

The previous correlations of Seban et al. [3], Dravid et al. [22], Rennie et al. [12] and Kozo et al. [23] in literature were also presented in Fig. 6. According to the comparison, it was found that the heat transfer coefficient on the outer surface of inner helical pipe was enlarged in helical annular duct, and the Nusselt number were higher than those in helical circular pipe. Less deviations were detected between the Nusselt numbers predicted by classical correlations and those obtained from experimental data, which meant the classical correlations could be employed for calculating the molten salt heat transfer coefficients on inner surface of outer pipe based on the thermal equivalent diameter.

3.3. Heat transfer characteristics of turbulent and transition regime

The Nusselt number of turbulent molten salt flow was plotted in Fig. 7. They indicated that the helical annular flow could also enhance the turbulent heat transfer coefficient. The Nusselt number on the outer wall of outer helical annular pipe was higher than that in helical circular pipe, and of course higher than those in straight circular pipe. For DTHHE #1 with smaller inner tube diameter and wider annular space, the heat transfer enhancement was more obvious, and the Nusselt number of the outer wall of the inner pipe was also larger than that of the inner wall of the outer pipe. For DTHHE #2 with larger inner tube diameter and wider annular space, the differences of Nusselt number between the outer wall of the inner pipe and the inner wall of the outer pipe decreased. The Nusselt number of outer wall become close to the prediction by Seban's correlation.

In this work, we used the following equation to correlation the variation of Nusselt number on inner wall:

$$Nu_t = C_1 Re^{C_2} Pr^{0.4} \left(\frac{d_T}{D_H}\right)^{C_3} \left(\frac{\mu_b}{\mu_w}\right)^{0.25} \tag{17}$$

The modification of varied viscosity was added to promote the accuracy of the correlation. Gnielinski [24] summarized convective heat transfer correlations in pipe, announced that the viscosity ratio in heat transfer correlation will be different during heating and cooling process, when fluid was cooled in pipe, the power of the viscosity should be 0.25. Thus there were three coefficients to be determined in above equation, i.e. C_1, C_2 and C_3. The coefficient of C_3 could be experimentally obtained by the comparison of heat transfer data in two types of helical annular ducts, and was calculated by the following equation:

$$C_3 = \frac{\ln(Nu_{\#1}/Nu_{\#2})}{\ln\left(\frac{d_{T,\#1}}{D_{H,\#1}}\cdot\frac{D_{H,\#2}}{d_{T,\#2}}\right)}, \quad (Re_{\#1} = Re_{\#2}, Pr_{\#1} = Pr_{\#2}) \tag{18}$$

where the $Nu_{\#1}$ and $Nu_{\#2}$ were Nusselt number of DTHHE #1 and DTHHE #2 with the same inlet Reynolds numbers and inlet

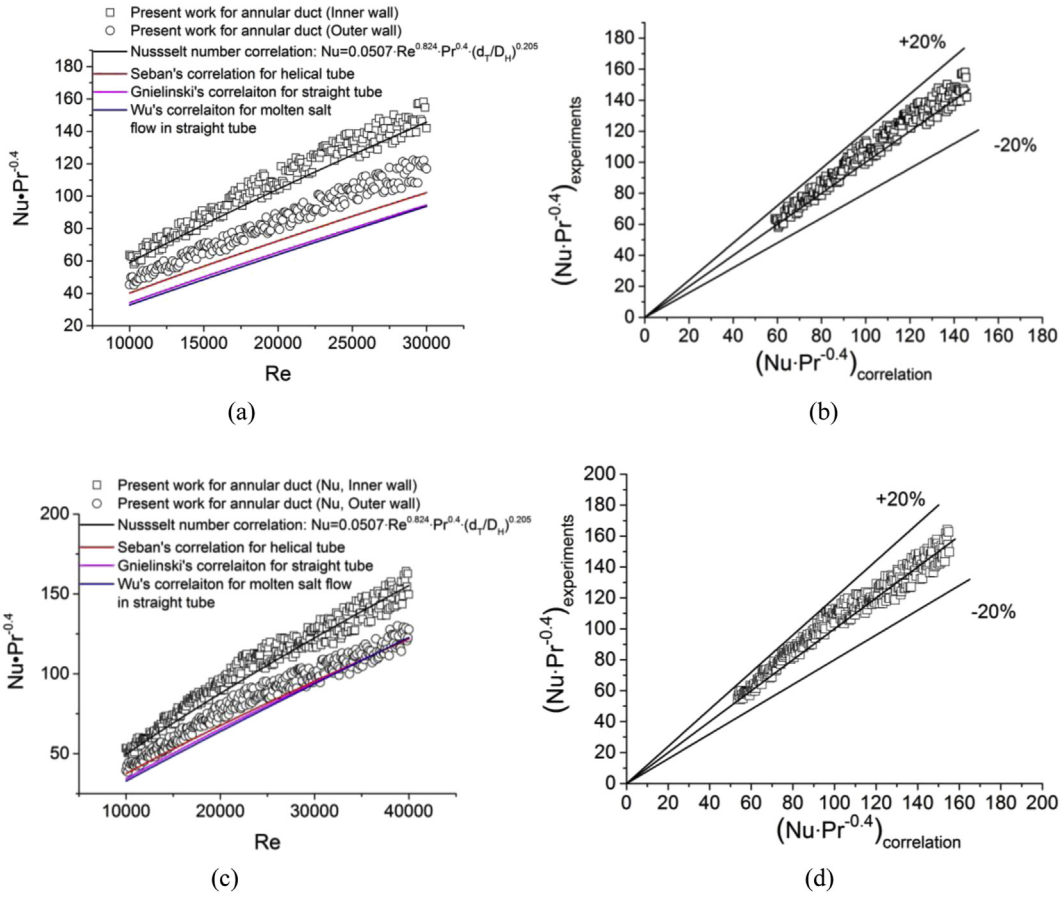

Fig. 7. The turbulent Nusselt numbers on inner and outer surface of helical annular duct versus various Reynolds number: (a) Nusselt number of DTHHE #1; (b) Deviation analysis for *Nu* correlation of DTHHE #1; (c) Nusselt number of DTHHE #2; (d) Deviation analysis for *Nu* correlation of DTHHE #2.

temperatures, respectively; the $d_{T,\#1}$ and $d_{T,\#2}$ were thermal equivalent diameters of DTHHE #1 and DTHHE #2, respectively; and the $D_{H,\#1}$ and $D_{H,\#2}$ represented the coil diameter of DTHHE #1 and DTHHE #2, respectively.

In the experiments, the coefficient of C_3 was firstly tested and determined as the averaged result of 0.205, with the largest deviation of 21.5%. Then the rest two coefficients of C_1 and C_2 could be calculated by the Wilson-Plot method with the similar calculating process of the laminar flow coefficients.

As a result, the correlation of molten salt turbulent flow in helical annular duct was obtained:

$$Nu_t = 0.0507 \cdot Re^{0.824} \cdot Pr^{0.4} \cdot \left(\frac{d_T}{D_H}\right)^{0.204} \left(\frac{\mu_b}{\mu_w}\right)^{0.25} \tag{19}$$

where, $10^4 < Re < 4 \times 10^4$, $Pr > 1$, $0.0312 < d_T/D_H < 0.0729$.

The deviations between the experimental data and correlation were also drawn in Fig. 7(b) and (d), the result shown good agreement of the proposed correlation in this work with the experimental data.

The Reynolds region of transition flow regime was short ($Re = 7 \times 10^3$~10^4), and the number of experimental data in transition region was much fewer than those of laminar and turbulent regime. Therefore the experimental results had too high deviation to be directly correlated. Churchill [25] analysed the essential heat transfer characteristics of transition flow regime, and indicated that the Nusselt correlation of transition region could be obtained according to the fully developed laminar correlation and fully developed turbulent correlation. Based on this theory, the transition correlations of molten salt were deduced as follows to connect the laminar and turbulent flow regimes:

$$Nu_{tr} = \left(\frac{1}{Nu_t^2} + \frac{1}{Nu_{lc}^2}\right)^{-1/2}, \quad Nu_{lc} = Nu_l \exp\left(\frac{Re - Re_{cr}}{300}\right), \quad Re_{cr} = 20{,}000 \times \left(\frac{d_T}{D_H}\right)^{0.32} \tag{20}$$

where, $Re_{cr} < Re < 10^4$, $Pr > 1$, $0.0312 < d_T/D_H < 0.0729$.

3.4. Heat transfer enhancement of molten salt flow in helical annular duct

The heat transfer enhancement was obtained for molten salt flowing in the helical annular duct. The heat transfer enhancement ratio was defined as the Nu_c/Nu_s, i.e. the ratio of the Nusselt number of helical annular duct to that of straight circular pipe.

The effects of molten salt temperature and helical annular duct structure were experimentally analysed. The heat transfer enhancement ratio (Nu_c/Nu_s) was employed for evaluating the enhanced heat transfer of molten salt in helical annular duct. The Nusselt number in straight tube was experimentally obtained in our work, the deviations of molten salt Nusselt numbers and the values predicted by empirical correlation were not significant, which were in agreement with the conclusions in previous literature [13,14]. Therefore the Nu_s was evaluated by the empirical equations for straight circular tube.

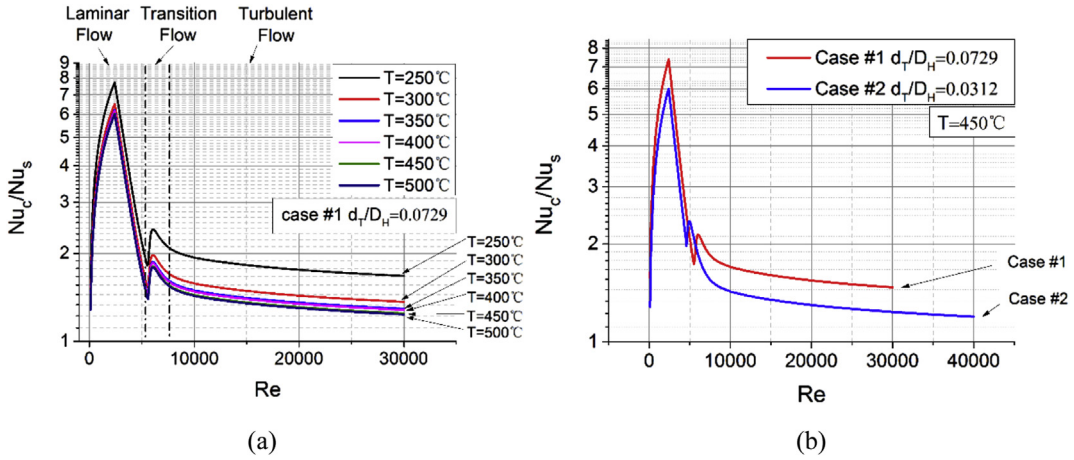

Fig. 8. The heat transfer ratios versus various molten salt flow Reynolds number: (a) the effect of molten salt temperature; (b) the effect of helical annular duct structure.

Fig. 8 showed the Nu_c/Nu_s distribution with various molten salt temperatures (250 °C–500 °C) and various helical annular duct structures (DTHHE #1 and DTHHE #2 in Table 1). It was found that the ratio of Nu_c/Nu_s was higher than unit and increased as the temperature of molten salt flow decreased, which indicated that the helical annular duct could enlarge the molten salt convective heat transfer compared with straight circular pipe, especially for the molten salt fluid with lower temperature. Furthermore, the laminar heat transfer enhancement ratios was found greater than those of turbulent and transition regime. The similar trend was also gained by previous researchers [22] using water as the working fluid. It could be explained as that the secondary flow could increase the velocity gradient beside the outer wall of the inner tube, which decreased the thickness of boundary layer and enlarged the molten salt heat transfer rate from core region to boundary layer region. Then better heat transfer performance was therefore caused. The contribution of the secondary flow to heat transfer in helical pipe was weakened with increasing Reynolds number [15]. Thus higher heat transfer enhancement ratio was obtained in laminar regime.

The heat transfer enhancement ratio of DTHHE #1 was higher than that of DTHHE #2, under the same Reynolds number. This trend verified the promoting effect of secondary flow on heat transfer coefficient and friction factor. According to the research results of Nobari [26] and Zhang [27], smaller inner-to-outer-pipe ratio ($\beta = r_i/r_o$) leads to additional vortices existing near the inner tube wall. The additional vortices reinforced secondary flow intensity, which further decreased the thickness of boundary layer and enlarged and caused higher heat transfer coefficients.

4. Conclusions

In this paper, the molten salt flowing in a helical annular duct was achieved, and the forced convective heat transfer characteristics of molten salt flow were experimentally studied. Following results were obtained:

1). The Darcy friction factor was obtained according to the pressure drop of molten salt flow in helical annular duct. The Darcy friction factor was found higher than that of helical circular pipe and that of straight circular pipe.
2). The laminar and turbulent flow regimes could be distinguished by the irregular change of Darcy friction factor. The critical Reynolds number by Ito's prediction in helical circular pipe was little higher than the experimental data in helical annular duct.
3). The laminar convective heat transfer correlation, turbulent correlation as well as transition correlation were obtained based on the thermal equivalent diameter. The result showed the good agreement with the experimental data, except the molten salt flow with very low velocity. When the Dean number was below 200, a great deviation was found, which was induced by the heat transfer enhancement of natural convection and could not be ignored.
4). The heat transfer enhancement were detected for molten salt flowing in helical annular duct. The ratio of Nu_c/Nu_s was found to be enlarged by smaller inner–outer-pipe diameter ratio and lower molten salt temperature.

Acknowledgements

This work was financially supported by the National Basic Research Program of China (Contracted No. 2009CB220000 and 2012CB215303) and the Natural Science Foundation of China (Contracted No. 51121092). The authors wish to thank Professor Chongfang Ma and Professor Yuting Wu, from Beijing University of Technology, for determining the thermal physical properties of molten salt.

References

[1] W.R. Dean, Fluid motion in a curved channel, Proc. Royal Soc. A Math. Phys. Eng. Sci. 121 (1928) 402–420.
[2] W.M. Kays, E.Y. Leung, Heat transfer in annular passages hydrodynamically developed turbulent flow with arbitrarily prescribed heat flux, Int. J. Heat Fluid Flow 6 (1962) 537–557.
[3] R.A. Seban, E.F. Mclaughlint, L.R. Labora, Heat transfer in tube coils with laminar flow and turbulent flow, Int. J. Heat Mass Transf. 6 (1963) 387–395.
[4] Y. Mori, W. Nakayama, Study on forced convective heat transfer in curved pipes (1st report, laminar region), Int. J. Heat Mass Transf. 8 (1965) 67–82.
[5] Y. Mori, W. Nakayama, Study on forced convective heat transfer in curved pipes (2nd report, turbulent region), Int. J. Heat Mass Transf. 10 (1967) 37–59.
[6] L.J. Guo, X.J. Chen, Z.P. Feng, B.F. Bai, Transient convective heat transfer in a helical coiled tube with pulsatile fully developed turbulent flow, Int. J. Heat Mass Transf. 41 (1998) 2867–2875.
[7] G.T. Karahalios, Mixed convection flow in a heated curved pipe with core, Phys. Fluids A Fluid Dyn. 2 (1990) 2164–2175.
[8] H.K. Choi, S.O. Park, Laminar entrance flow in curved annular ducts, Int. J. Heat Mass Transf. 13 (1992) 41–49.
[9] S. Garimella, D.E. Richards, R.N. Christensen, Experimental investigation of heat transfer in coiled annular ducts, J. Heat Transf. 110 (1988) 329–336.
[10] R.C. Xin, A. Awwad, Z.F. Dong, M.A. Ebadian, An experimental study of single-phase and two-phase flow pressure drop in annular helicoidal pipes, Int. J. Heat Fluid Flow 18 (1997) 482–488.
[11] H.J. Kang, C.X. Lin, M.A. Ebadian, Condensation of R134a flowing inside helicoidal pipe, Int. J. Heat Mass Transf. 43 (2000) 2553–2564.

[12] T.J. Rennie, V.G.S. Raghavan, Experimental studies of a double-pipe helical heat exchanger, Exp. Therm. Fluid Sci. 29 (2005) 919–924.
[13] Y.T. Wu, C. Chen, B. Liu, C.F. Ma, Investigation on forced convective heat transfer of molten salts in circular tubes, Int. Commun. Heat Mass Transf. 39 (2012) 1550–1555.
[14] B. Liu, Y.T. Wu, C.F. Ma, M. Ye, H. Guo, Turbulent convective heat transfer with molten salt in a circular pipe, Int. Commun. Heat Mass Transf. 36 (2009) 912–916.
[15] Y.F. Mao, L.J. Guo, B.F. Bai, Pressure drop and heat transfer to turbulent flow of supercritical pressure water in a vertical-upward helically-coiled tube, in: 7th International Conference on Multiphase Flow, Tampa, USA, 2010.
[16] W.L. Chen, Y.C. Yang, W.J. Chang, H.L. Lee, Inverse problem of estimating transient heat transfer rate on external wall of forced convection pipe, Energy Convers. Manage. 49 (2008) 2117–2123.
[17] J. Fernández-Seara, F.J. Uhía, J. Sieres, A. Campo, A general review of the Wilson plot method and its modifications to determine convection coefficients in heat exchange devices, Appl. Therm. Eng. 27 (2007) 2745–2757.
[18] S. Liu, A. Afacan, H.A. Nasr-El-Din, J.H. Masliyah, An experimental study of pressure drop in helical pipes, Proc. Royal Soc. Lond. Ser. A Math. Phys. Sci. 444 (1994) 307–316.
[19] H. Ito, Friction factors for turbulent flow in curved pipes, ASME J. Basic Eng. 81 (1959) 123–134.
[20] M.A. Petrakis, G.T. Karahalios, Steady flow in a curved pipe with a coaxial core, Int. J. Numer. Methods Fluids 22 (1996) 1231–1237.
[21] K.N. Ghia, J.S. Sokhey, Laminar incompressible viscous flow in curved ducts of regular cross-sections, J. Fluids Eng. 99 (1977) 640–648.
[22] A.N. Dravid, K.A. Smith, E.W. Merrill, P.L.T. Brian, Effect of secondary fluid motion on laminar flow heat transfer in helically coiled tubes, AIChE J. 17 (1971) 1114–1122.
[23] K. Futagami, I. Engineering, Laminar heat transfer in a helically coiled tube, Int. J. Heat Mass Transf. 31 (1988) 387–396.
[24] V. Gnielinski, New equations for heat and mass transfer in the turbulent flow in pipes and channels, Forsch. Im. Ingenieurwes. 41 (1975) 8–16.
[25] S.W. Churchill, Comprehensive correlating equations for heat, mass and momentum transfer in fully developed flow in smooth tubes, Ind. Eng. Chem. Fundam. 16 (1977) 109–116.
[26] M.R.H. Nobari, A. Malvandi, Torsion and curvature effects on fluid flow in a helical annulus, Int. J. Non-Linear Mech. 57 (2013) 90–101.
[27] J. Zhang, B. Zhang, H. Chen, Flow in helical annular pipe, J. Eng. Mech. 126 (2000) 1040–1047.

Nomenclature

A: area (m^2)
C_p: thermal capacity (J/kg K)
D_H: coil diameter (m)
De: Dean number (−)
d_T: thermal equivalent diameter (m). $d_{T,i} = [(d_o^i)^2 - (d_i^o)^2]q_i/(d_o^i q_o + d_i^o q_i)$
$d_{T,o} = [(d_o^i)^2 - (d_i^o)^2]q_o/(d_o^i q_o + d_i^o q_i)$
f: Darcy friction factor (−)
g: gravitational acceleration (m^2/s)
H: enthalpy (J/kg)
h: heat transfer coefficient (W/m^2 K)
k: overall heat transfer coefficient (W/m^2 K)
L: length (m)
M: mass flow rate (kg/s)
Nu: Nusselt number (−)
n: coil number (−)
P: pressure (pa)
Pr: Prandtl number (−)
q: heat flux (W/m^2)
Re: Reynolds number
r: radius (m)
T: temperature (K)
v: velocity (m/s)

Greek symbols

β: inner to outer diameter ratio
γ: kinetic viscosity (m^2/s)
ε: temperature difference due to heat loss (K)
λ: thermal conductivity (W/m K)
μ: dynamic viscosity (Pa s)
ρ: density (kg/m^3)

Subscripts

0: initial
H: helical
i: inner pipe
MS: molten salt
o: outer pipe
T: thermal equivalent
W: water

Superscripts

i: inner wall
o: outer wall